High resolution infrared emission spectra of GaH and GaD

J. M. Campbell, M. Dulick, D. Klapstein,[a] J. B. White, and P. F. Bernath
Centre for Molecular Beams and Laser Chemistry, Department of Chemistry, University of Waterloo, Waterloo, Ontario N2L 3G1, Canada

(Received 8 June 1993; accepted 17 August 1993)

The high resolution infrared emission spectra of gallium hydride and gallium deuteride have been recorded with a Fourier transform spectrometer. There were 1045 lines observed including those from the $v=1\rightarrow0$ to $v=7\rightarrow6$ bands for the ^{69}GaD and ^{71}GaD species and $v=1\rightarrow0$ to $v=4\rightarrow3$ bands for the ^{69}GaH and ^{71}GaH species. Dunham Y_{ij}'s for each isotopomer were obtained by fitting the data set of each isotopomer separately to the Dunham energy levels of the $X\,^1\Sigma^+$ electronic ground state. The mass-reduced Dunham U_{ij}'s were determined using two independent methods. In the first fit the U_{ij}'s constants were determined by the traditional method where all the constants were treated as adjustable parameters and determined statistically. In the second fit the U_{ij}'s which satisfied the condition $j<2$ were treated as adjustable parameters and the remaining constants were fixed by constraints imposed by the Dunham model. In order to predict the positions of transitions with v's and J's much higher than those observed the entire data set was fit directly to the eigenvalues of the Schrödinger equation containing a parameterized internuclear potential energy function.

I. INTRODUCTION

In contrast to isovalent aluminum hydride,[1] relatively few spectroscopic studies have been reported for gallium hydride and deuteride. Garton ascribed bands observed in the 2160–2400 Å region of the spectrum to GaH.[2] Since then there have been several classical spectroscopic studies reported that have focused mainly on the analysis of bands involving the nominally forbidden $a\,^3\Pi$–$X\,^1\Sigma^+$ intercombination transitions of GaH and GaD.

Neuhaus recorded and analyzed the 0–0 bands of the GaH $a\,^3\Pi_1$–$X\,^1\Sigma^+$ and $a\,^3\Pi_{0+}$–$X\,^1\Sigma^+$ transitions and the GaD $a\,^3\Pi_1$–$X\,^1\Sigma^+$ transition.[3,4] In a subsequent study he observed predissociation in the $A\,^1\Pi$–$X\,^1\Sigma^+$ transitions of GaH and GaD, but only the lines in the spectrum of GaD were sharp enough for rotational analysis.[5] Ginter and Innes[6] analyzed 16 bands of GaH including some bands of previously unobserved $a\,^3\Pi_2$–$X\,^1\Sigma^+$ and doubly forbidden $a\,^3\Pi_{0-}$–$X\,^1\Sigma^+$ transitions.[7] More recently Lakshminarayana and Shetty formed GaD by exciting a mixture of gaseous gallium metal, iodine vapor, deuterium, and krypton in a microwave discharge and rotationally analyzed several emission bands of the GaD $a\,^3\Pi_1$–$X\,^1\Sigma^+$, $a\,^3\Pi_{0+}$–$X\,^1\Sigma^+$, and $a\,^3\Pi_{0-}$–$X\,^1\Sigma^+$ transitions.[8]

Results from theoretical studies on GaH and GaD are also available. Ginter and Battino applied the Rydberg–Klein–Rees (RKR) method to obtain potential energy curves for the $a\,^3\Pi$ and $X\,^1\Sigma^+$ states of selected Group IIIa hydrides, including GaH.[9] Pettersson and Langhoff have calculated the theoretical electric-dipole moment and dissociation energy for the $X\,^1\Sigma^+$ electronic ground state of GaH.[10] The multiconfiguration self-consistent field (MCSCF) [complete active space SCF (CASSCF)] calculation by Kim and Balasubramanian yielded potential energy curves, spectroscopic constants, and dipole-moment functions for 25 electronic states of GaH, of which 17 of these states have yet to be observed.[11]

More recently, Jones and co-workers[12,13] recorded high resolution vibrational-rotational spectra for the GaH and GaD $X\,^1\Sigma^+$ ground states using diode laser spectroscopy. GaH (GaD) was formed in a high temperature reaction involving molten gallium and hydrogen (deuterium). The recorded line positions were reduced to Dunham Y_{ij} constants and potential parameters. However, they were able to measure relatively few rovibrational transitions and they covered a narrow spectral range due to the limited tunability of diode lasers. They reported $\sim$100 lines with a nominal accuracy of 0.001 cm^{-1}.

As noted by Jones and co-workers, the simultaneous analysis of the rovibrational spectra of the Group IIIa diatomic hydrides and deuterides provides an excellent way of determining the extent of Born–Oppenheimer breakdown.[13] Gallium has two naturally occurring isotopes, ^{69}Ga (60.2%) and ^{71}Ga (39.2%). The simultaneous analysis of GaH and GaD spectra yields data of comparable quality for the four different isotopomers, thus allowing the effects of Born–Oppenheimer breakdown to be examined for both nuclear centers.

In this paper we report on the analysis of the infrared (IR) emission spectra of GaH and GaD recorded with a Fourier transform spectrometer. Although this technique lacks the sensitivity of tunable diode laser spectroscopy, it does, however, provide wide spectral coverage and highly accurate rovibrational line positions. We observed over 1000 lines in the GaH and GaD spectra with the best lines being measured to a precision of ±0.0002 cm^{-1}. The reduction of the data set to spectroscopic constants was accomplished by fitting the data separately to the energy levels of the Dunham model and a parameterized potential energy model.

[a]Permanent address: Chemistry Department, Saint Francis Xavier University, Antigonish, N.S. B2G 1C0, Canada.

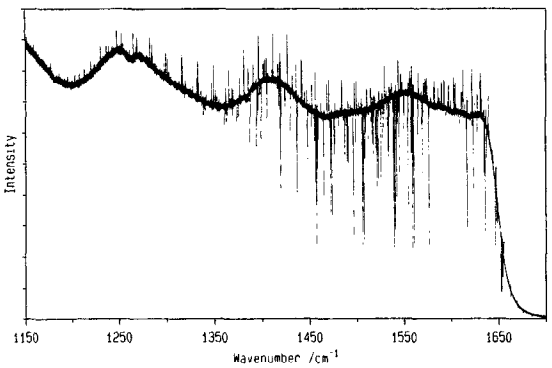

FIG. 1. Overview of the high resolution infrared emission spectrum of GaH recorded with KBr windows and beamsplitter.

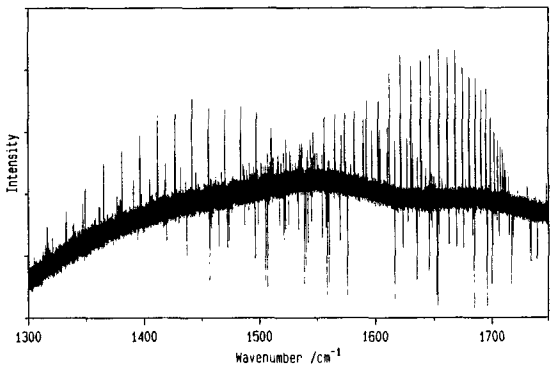

FIG. 2. Overview of the high resolution infrared emission spectrum of GaH recorded with CaF_2 windows and beamsplitter.

II. EXPERIMENT

All spectra were recorded on a Bruker IFS 120 HR spectrometer at the University of Waterloo. A total of three high resolution spectra were recorded, two for GaH and one for GaD. In order to record each spectrum, 12 g of gallium metal was placed in the center of a 1.2 m long mullite ($3Al_2O_3 \cdot 2SiO_2$) tube with heat supplied by a tube furnace. The mullite cell was located external to the spectrometer and aligned to the emission port through the use of an external globar lamp. The apparatus is described in greater detail elsewhere.[14–16] The Ga in the mullite tube was gradually heated to operating temperature at a rate of ~ 5 °C/min and when a temperature of 500 °C was achieved, the pumping port was closed, and 5 Torr of argon gas was added to the system to prevent the deposition of solid material on the cell windows. At 1200 °C hydrogen or deuterium was added to the cell. All high resolution spectra were recorded at 1400 °C.

A HgCdTe detector was used to record all spectra. Each high resolution spectrum involved the coaddition of 75 individual scans each recorded at a resolution of 0.007 cm^{-1}. The GaD spectrum and one of two GaH spectra were recorded using a KBr beamsplitter and KBr windows. In these spectra the lower wave-number limit of 800 cm^{-1} was dictated by detector sensitivity while the 1700 cm^{-1} upper limit was set by a short wavelength cutoff filter. As is evident in Fig. 1, the bandhead of the GaH fundamental band ($v=1\rightarrow 0$) lies beyond the 1700 cm^{-1} upper cutoff limit. In order to record the band head region of the GaH fundamental band the 1700 cm^{-1} upper wave-number cutoff filter was replaced with a 2200 cm^{-1} upper wave-number cutoff filter. In addition the KBr beamsplitter and KBr windows were replaced with a CaF_2 beamsplitter and CaF_2 windows; the CaF_2 transmission curve raises the lower wave-number limit to 1150 cm^{-1}.

III. RESULTS AND DISCUSSION

Data analysis was facilitated using the PC-DECOMP computer program of Brault which determines line positions by fitting measured line profiles to Voigt line shape functions. Absolute wave number calibration of the GaH line positions was achieved by utilizing impurity H_2O lines in the spectrum.[17]

Portions of the two high resolution GaH spectra are displayed in Figs. 1 and 2. In the spectrum shown in Fig. 1, the bands $v=1\rightarrow 0$ to $v=4\rightarrow 3$ were observed and the sharp and unblended lines with a signal to noise (S/N) ratio greater than 100 were measured to a precision of ± 0.0003 cm^{-1}. The lower S/N ratio in the spectrum of Fig. 2 degraded the precision of the measured line centers of the strong and unblended lines to ± 0.0005 cm^{-1}. Initially, each of the GaH spectra was independently calibrated relative to the strongest and sharpest H_2O lines. However, calibrating the spectra in this manner introduced a systematic shift of 0.0002 cm^{-1} between lines common to both spectra. In order to place the measured rotational lines from both spectra on the same absolute wave-number scale, thereby circumventing any systematic shift in the calibration between spectra, we were forced to adopt the following calibration procedure. The strongest GaH rotational lines from the first spectrum (the best of the two spectra in terms of S/N) were calibrated relative to H_2O lines and these GaH lines were used to calibrate the remaining lines in both spectra.

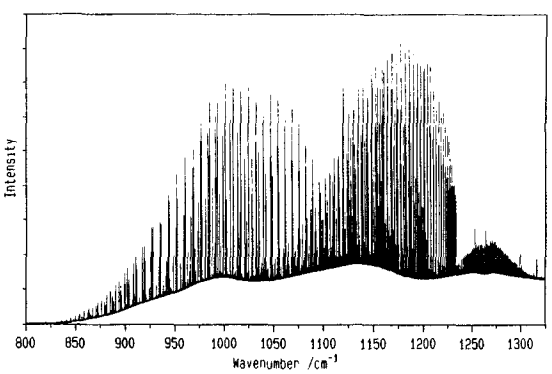

FIG. 3. Overview of the high resolution infrared emission spectrum of GaD.

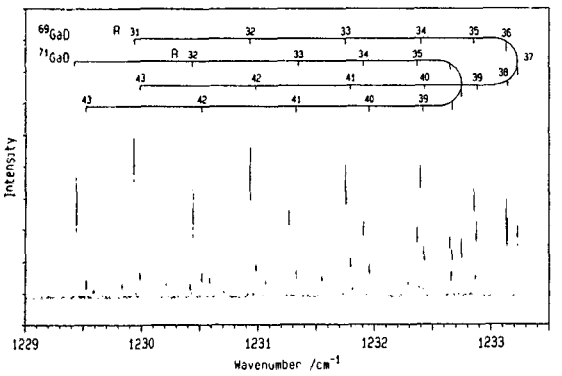

FIG. 4. Details of the bandhead region of $v=1\rightarrow0$ band of GaD. Lines not labeled are those of the impurity SiO.

The quality of the GaD spectrum is illustrated in Figs. 3 and 4. The vibrational bands that were observed are $v=1\rightarrow0$ to $v=7\rightarrow6$. All rotational lines in the GaD spectrum were calibrated relative to H_2O lines. Rotational lines of GaH present in the GaD spectrum were then used to verify that the GaH and GaD spectra were in fact on the same wave number scale. Although the internal consistency between measured lines in both the GaH and GaD spectra is perhaps as good as ±0.0001 cm^{-1}, the error in the absolute calibration (with H_2O lines serving as the source of calibration) is difficult to ascertain without additional independent measurements.

The observed rotational lines for ^{69}GaH, ^{71}GaH, ^{69}GaD, and ^{71}GaD are available from PAPS,[18] or from the authors on request. Each of the four isotopomer data sets was separately fit to the parameterized energy levels of the Dunham model[19]

$$E(v,J)=\sum_{i,j}Y_{ij}(v+\tfrac{1}{2})^i[J(J+1)]^j, \tag{1}$$

where v and J are the vibrational and rotational quantum numbers. The Dunham Y_{ij} constants for each isotopomer are given in Table I. Since our IR data set was able to access vibrational-rotational levels almost up to 50% of the potential well depth the new Dunham constants Y_{41}, Y_{32}, Y_{23}, and Y_{04} for both GaH and GaD and Y_{50} and Y_{13} for GaD were determined. In addition, the high quality of our data set also lead to improving the precision of the Dunham constants quoted by Urban *et al.*[12,13]

Explicitly factoring the reduced-mass dependence out of Y_{ij} gives the equation

$$E(v,J)=\sum_{i,j}\mu^{-(i+2j)/2}U_{ij}(v+\tfrac{1}{2})^i[J(J+1)]^j. \tag{2}$$

Equation (2) is strictly valid only within the Born–Oppenheimer approximation. In the case of Born–Oppenheimer breakdown, Eq. (2) is modified as[20,21]

$$E(v,J)=\sum_{i,j}\mu^{-(i+2j)/2}U_{ij}(v+\tfrac{1}{2})^i[J(J+1)]^j \times\left(1+\frac{m_e}{M_A}\Delta_{ij}^A+\frac{m_e}{M_B}\Delta_{ij}^B\right), \tag{3}$$

where m_e is electron mass, M_A and M_B are atomic masses for centers A and B, and Δ_{ij} are Born–Oppenheimer breakdown constants. Values of the U_{ij}'s and Δ_{ij}'s determined from a least-squares fit of all the isotopomer data to Eq. (3) are given in Table II under the column heading "unconstrained fit." The standard deviation of the fit was 0.642.

A further refinement to the Dunham model entails the placement of constraints on the U_{ij}'s for $j\geqslant2$.[16] Dunham has shown that the potential parameters for a power series potential are all uniquely determined by the set of U_{i0}'s and U_{i1}'s. Consequently, the remaining U_{ij}'s with $j\geqslant2$ are all expressible in terms of U_{i0}'s and U_{i1}'s. For the purpose of least-squares fitting, the U_{i0}'s and U_{i1}'s are treated as ad-

TABLE I. Dunham Y_{ij} constants of ^{69}GaH, ^{71}GaH, ^{69}GaD, and ^{71}GaD.

Y_{ij}	^{69}GaH	^{71}GaH	^{69}GaD	^{71}GaD
Y_{10}	1 603.940 94(57)	1 603.612 94(73)	1 143.227 36(13)	1 142.769 38(18)
Y_{20}	−28.410 821(520)	−28.397 560(657)	−14.425 947 4(994)	−14.414 110(138)
Y_{30}	0.324 166(182)	0.323 468(227)	0.116 383 1(315)	0.116 163 6(454)
10^3Y_{40}	−6.654 5(216)	−6.600 4(264)	−1.583 91(446)	−1.573 18(661)
10^6Y_{50}	...	...	−7.156(231)	−7.338(353)
Y_{01}	6.143 409 51(372)	6.140 908 83(548)	3.121 885 40(81)	3.119 390 44(112)
Y_{11}	−0.190 637 61(523)	−0.190 507 11(712)	−0.068 997 844(400)	−0.068 914 161(526)
10^3Y_{21}	2.750 17(435)	2.737 83(586)	0.709 005(158)	0.707 051(227)
10^5Y_{31}	−4.264(147)	−4.054(195)	−0.808 68(279)	−0.788 38(440)
10^6Y_{41}	−1.640(173)	−1.750(224)	−0.184 47(176)	−0.198 00(301)
10^4Y_{02}	−3.596 961(193)	−3.593 712(288)	−0.930 208 9(146)	−0.928 731 0(230)
10^6Y_{12}	8.616 37(961)	8.582 0(129)	1.580 546(602)	1.577 578(813)
10^8Y_{22}	−8.707(387)	−6.956(535)	−1.019 3(113)	−0.983 6(151)
10^8Y_{32}	−1.048 6(483)	−1.277 5(699)	−0.103 896(795)	−0.106 90(116)
10^8Y_{03}	1.351 25(385)	1.346 22(597)	0.180 331(121)	0.179 705(209)
$10^{10}Y_{13}$	−1.591 9(797)	−1.551(108)	−0.129 24(320)	−0.134 20(474)
$10^{11}Y_{23}$	−2.628(200)	−3.044(285)	−0.214 03(357)	−0.216 44(501)
$10^{13}Y_{04}$	−4.777(255)	−4.653(413)	−0.394 11(578)	−0.375 98(984)

TABLE II. (a) Mass-reduced Dunham constants for GaH in cm^{-1}. See text for an explanation of constrained and unconstrained fits. (b) Born–Oppenheimer breakdown constants from constrained and unconstrained fits.

	U_{ij}	Unconstrained	Constrained
(a)	U_{10}	1 599.962 47(52)	1 599.962 01(60)
	U_{20}	−28.245 656(171)	−28.245 050(183)
	U_{30}	0.318 698 6(762)	0.318 363 5(835)
	10^3U_{40}	−6.063 6(154)	−5.980 8(170)
	10^5U_{50}	−3.808(114)	−4.574(124)
	U_{01}	6.116 430 5(170)	6.116 362 9(139)
	U_{11}	−0.189 047 313(986)	−0.189 047 269(463)
	10^3U_{21}	2.714 353(670)	2.718 181(279)
	10^5U_{31}	−4.272 6(214)	−4.416 16(852)
	10^6U_{41}	−1.451 5(234)	−1.290 07(986)
	10^4U_{02}	−3.575 287(109)	−3.575 365 09
	10^6U_{12}	8.499 37(202)	8.482 992 75
	10^8U_{22}	−7.558(104)	−7.746 592 66
	10^8U_{32}	−1.183 5(334)	−1.100 896 93
	$10^{10}U_{42}$	1.067(399)	−0.056 310 182 3
	10^8U_{03}	1.363 04(116)	1.363 641 03
	$10^{10}U_{13}$	−1.551 1(150)	−1.262 721 28
	$10^{11}U_{23}$	−2.915 9(338)	−2.976 361 59
	$10^{13}U_{33}$	···	4.975 760 99
	$10^{13}U_{04}$	−5.249 2(382)	−5.640 813 65
	$10^{14}U_{14}$	···	−1.446 105 59
	$10^{16}U_{24}$	···	−5.533 977 44
	$10^{16}U_{34}$	···	−2.420 216 00
	$10^{17}U_{05}$	···	3.353 474 98
	$10^{18}U_{15}$	···	−2.279 294 18
	$10^{19}U_{25}$	···	1.463 910 77
	$10^{21}U_{06}$	···	−2.507 282 89
	$10^{23}U_{16}$	···	7.526 568 81
	$10^{23}U_{26}$	···	−8.986 782 30
	$10^{25}U_{07}$	···	1.046 169 47
	$10^{27}U_{17}$	···	1.148 245 38
	$10^{30}U_{08}$	···	−7.632 001 67
	$10^{30}U_{18}$	···	−5.573 709 40
	$10^{34}U_{09}$	···	5.509 323 79
	$10^{38}U_{010}$	···	−9.048 761 69
(b)	Δ_{10}^{Ga}	0.244 6(389)	0.238 3(456)
	Δ_{01}^{Ga}	−2.621(347)	−1.081(259)
	Δ_{10}^{H}	−1.620 469(221)	−1.620 226(257)
	Δ_{20}^{H}	−1.994 02(650)	−1.983 79(756)
	Δ_{30}^{H}	−1.451 2(912)	−1.216(105)
	Δ_{01}^{H}	−4.218 05(132)	−4.218 388(769)
	Δ_{11}^{H}	−3.141 39(748)	−3.119 25(547)
	Δ_{21}^{H}	−0.580 1(778)	−0.628 7(846)
	Δ_{02}^{H}	−13.378 1(765)	−13.296 9(201)
	Δ_{12}^{H}	−7.982(264)	−6.670 8(813)
	Δ_{03}^{H}	−41.08(198)	−36.934(273)

justable parameters with all remaining U_{ij}'s fixed to values satisfying these constraints. Results from fitting the GaH and GaD data to this model using the constrained U_{ij} relations that were derived by Ogilvie[22] are also listed in Table II under the column heading "constrained." With 21 adjustable parameters the standard deviation of this fit was 0.761 or 19% higher than the standard deviation of the unconstrained fit with 30 adjustable parameters.

To obtain information on the high lying v, J levels of the ground state a reliable internuclear potential energy function is required. Such a potential function can be obtained directly by using the method referred to by us as the parameterized potential model.[23] Our technique is similar to the procedure developed by Coxon and Hajigeorgiou.[24,25] Specifically, the method involves fitting spectral lines directly to the eigenvalues of the radial Schrödinger equation containing a parameterized potential function. With the effective radial Schrödinger equation for the $^1\Sigma^+$ state of a diatomic molecule written as

$$\left\{\frac{\hbar^2}{2\mu}\nabla^2 - U^{\text{eff}}(R) + E(v,J) - \frac{\hbar^2}{2\mu}[1+q(R)]\frac{J(J+1)}{R^2}\right\} \times \psi(r;v,J) = 0, \tag{4}$$

the effective internuclear potential for vibrational motion is given by

$$U^{\text{eff}}(R) = U^{\text{BO}}(R) + \frac{U_A(R)}{M_A} + \frac{U_B(R)}{M_B}, \tag{5}$$

and the form of the Born–Oppenheimer potential is chosen to be

$$U^{\text{BO}}(r) = D_e\left[\frac{1-e^{-\beta(R)}}{1-e^{-\beta(\infty)}}\right]^2, \tag{6}$$

where

$$\beta(R) = z\sum_{i=0}\beta_i z^i, \tag{7}$$

$$\beta(\infty) = \sum_{i=0}\beta_i, \tag{8}$$

and

$$z = \frac{(R-R_e)}{(R+R_e)}, \tag{9}$$

is one-half the Ogilvie–Tipping parameter.

The latter terms in Eq. (5) are corrections for atomic centers A and B which take into account Born–Oppenheimer breakdown and homogeneous nonadiabatic mixing from distant Σ electronic states and are represented by the power series expansions

$$U_A(R) = \sum_{j=1} u_i^A(R-R_e)^i \tag{10}$$

and

$$U_B(R) = \sum_{i=1} u_i^B(R-R_e)^i. \tag{11}$$

Similar effects for rotational motion, namely J-dependent Born–Oppenheimer breakdown and heterogenous nonadiabatic mixing from distant Π states, are accounted for through the inclusion of the $q(R)$ term in Eq. (4) where

$$q(R) = M_A^{-1}\sum_{i=1} q_i^A(R-R_e)^i + M_B^{-1}\sum_{i=1} q_i^B(R-R_e)^i. \tag{12}$$

Results from the fit of the GaH and GaD data to the parameterized potential model are given in Table III. The potential energy function is plotted in Fig. 5. The standard deviation of the fit was 0.811. Parameters that were statis-

TABLE III. Internuclear potential parameters. Values of u_i^A given are in cm^{-1} $Å^{-i}$ and values of q_i^A are given in $Å^{-i}$.

Parameter	Value	Uncertainty
$10^{-4}D_e$ (cm^{-1})	2.29	
R_e (Å)	1.660 130 365 553 748	4.75×10^{-7}
β_0	4.275 027 073 887 386	1.80×10^{-6}
β_1	3.376 962 034 094 690	2.27×10^{-5}
β_2	6.417 723 606 340 825	2.55×10^{-4}
β_3	13.879 380 707 128 89	3.05×10^{-3}
β_4	25.819 625 651 843 39	2.97×10^{-2}
β_5	53.791 352 147 482 69	2.07×10^{-1}
β_6	84.889 069 770 902 58	1.29×10^{0}
β_7	−435.807 384 478 536 6	6.32×10^{0}
β_8	673.234 544 141 024 7	1.03×10^{1}
β_9	7 916.002 626 552 201	1.82×10^{1}
u_1^{Ga}	−210.097 923 884 167 4	2.38×10^{0}
u_2^{Ga}	420.749 632 972 798 6	3.61×10^{0}
u_3^{Ga}	−259.153 857 115 170 9	3.79×10^{0}
u_4^{Ga}	−45.943 186 146 578 39	4.33×10^{0}
u_1^{H}	−146.378 106 672 391 1	2.15×10^{-2}
u_2^{H}	245.109 248 175 388 4	4.64×10^{-2}
u_3^{H}	−288.867 111 344 353 4	7.61×10^{-1}
u_4^{H}	289.062 574 407 010 3	2.35×10^{0}
u_5^{H}	−235.502 054 034 798 5	3.28×10^{0}
u_6^{H}	94.947 441 008 322 98	3.31×10^{0}
u_7^{H}	43.800 669 635 260 11	2.99×10^{0}
u_9^{H}	−59.708 793 578 546 26	1.89×10^{0}
q_1^{H}	0.001 365 884 770 872 012	3.46×10^{-6}
q_2^{H}	−0.002 386 554 965 271 707	3.30×10^{-5}
q_3^{H}	0.002 680 865 123 078 248	3.99×10^{-5}
q_4^{H}	−0.003 021 063 706 719 714	9.74×10^{-5}
q_5^{H}	0.001 785 099 884 560 774	1.10×10^{-4}
M_{Ga} (^{69}Ga)	68.925 580	
M_{Ga} (^{71}Ga)	70.924 700 5	
M_H (^{1}H)	1.007 825	
M_H (^{2}H)	2.014 101 779	

tically determined are listed along with their uncertainties quoted to one standard deviation. The thermochemical value for the dissociation energy D_e was taken from Ref. 26 and quoted atomic masses from Ref. 27.

The constrained and unconstrained Dunham U_{ij} constants in Table II are for the most part in agreement to within three standard deviations. This indicates that effects ascribed to perturbations with higher lying electronic states are essentially insignificant. It is worth noting that Δ_{10}^{Ga} and Δ_{01}^{Ga} from the unconstrained and constrained fits are just barely determined to three standard deviations. On the other hand, a disproportionate number of Δ's are well determined from both fits for the hydrogen center; this is consistent with the atomic mass of the gallium atom contributing only 1.4% (2.8%) to the reduced mass of the diatomic hydride (deuteride) molecule. Therefore, the immediate conclusion that one can draw from these results is that the contribution of Born–Oppenheimer breakdown by the gallium metal center is essentially insignificant.

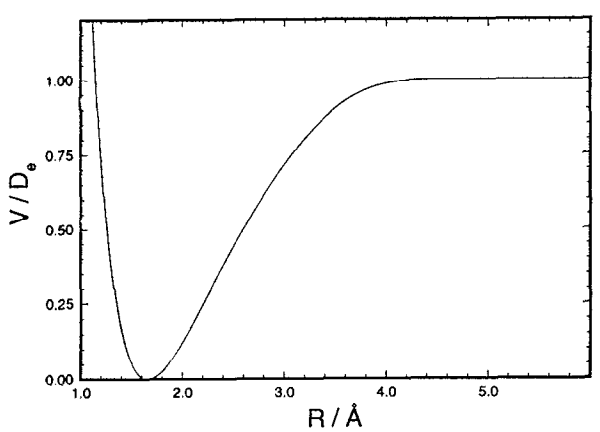

FIG. 5. The Born–Oppenheimer potential for GaH.

Results from the parameterized potential model fit serve as a cross check on the conventional treatment of Born–Oppenheimer breakdown given by Eq. (3). According to Coxon and Hajigeoriou,[24]

$$\Delta_{01}^{i}\simeq 2(m_e k^{BO} R_e^{BO})^{-1}\left[\frac{dU_i(R)}{dR}\right]_{R=R_e^{BO}}, \tag{13}$$

where i is A or B and

$$k^{BO}=\left[\frac{d^2U^{BO}(R)}{dR^2}\right]_{R=R_e^{BO}} \tag{14}$$

is the harmonic force constant for the Born–Oppenheimer potential. [Strict equality applies only if a small Dunham correction is added to the right-hand side of Eq. (13).] Substituting Eq. (10) [or Eq. (11)] into Eq. (13) and Eq. (6) into Eq. (14) gives

$$\Delta_{01}^{i}\simeq\frac{4R_e^{BO}[1-e^{-\beta(\infty)}]^2}{D_e\beta_0^2 m_e}u_1^i. \tag{15}$$

Using the parameter values in Table III yield the values, $\Delta_{01}^{Ga}=-6.077(69)$ and $\Delta_{01}^{H}=-4.233\,75(62)$. Adding the small Dunham correction to these values give $\Delta_{01}^{Ga}=-6.059(69)$ and $\Delta_{01}^{H}=-4.215\,95(62)$. By comparing these values to the ones listed in Table II shows that only the Δ_{01}^{H}'s are in good agreement whereas the value of Δ_{01}^{Ga} from the constrained Dunham fit is almost a factor of 6 smaller than the value derived from the analysis presented here.

The discrepancy in the Δ_{01}^{Ga}'s can be explained as follows. With the Eq. (3) multiplicative factor

$$1+\frac{m_e}{M_{Ga}}\Delta_{01}^{Ga}+\frac{m_e}{M_H}\Delta_{01}^{H}, \tag{16}$$

that corrects for Born–Oppenheimer breakdown and the corrected values of Δ_{01}^{Ga} and Δ_{01}^{H} quoted above yield the values

$$\frac{m_e}{M_{^{69}Ga}}\Delta_{01}^{Ga}=-0.000\,048\,2,$$

$$\frac{m_e}{M_{^{71}Ga}}\Delta_{01}^{Ga}=-0.000\,046\,8,$$

$$\frac{m_e}{M_H}\Delta_{01}^{H}=-0.002\,294\,8,$$

$$\frac{m_e}{M_D}\Delta_{01}^{H} = -0.001\,148\,2,$$

for the terms in Eq. (16). One can immediately see that the Δ_{01}^{Ga} term is fairly insensitive to change in isotopic mass and is almost two orders of magnitude smaller than the Δ_{01}^{H} term. These two properties in combination with high correlation between Δ_{01}^{Ga} and U_{01} in a least-squares fit hinder the determination of Δ_{01}^{Ga} to a much greater extent than for Δ_{01}^{H}. Therefore, the form of the Born–Oppenheimer correction given by Eq. (16) is an insensitive way of determining metal-centered Δ's from a least-squares fit when the diatomic molecule is a heavy-metal hydride.

IV. CONCLUSION

Fourier transform emission spectroscopy is an excellent technique for recording high resolution vibrational-rotational spectra of high temperature molecules in the infrared region. As is evident in this work presented on GaH and GaD, this technique gives broad spectral coverage and an excellent S/N ratio thus making it possible to record a significant number of line positions with high precision. The high quality of line positions makes the data set particularly useful in the determination of spectroscopic constants and internuclear potentials.

The four isotopomer data sets, ^{69}GaH, ^{71}GaH, ^{69}GaD, and ^{71}GaD, were fit individually to the energy levels of the Dunham model to determine Dunham Y_{ij}'s and combined together in a fit to determine the mass-independent Dunham U_{ij}'s. A second set of U_{ij}'s was determined from a fit where the U_{i0}'s and U_{i1}'s were treated as adjustable parameters and the remaining U_{ij}'s were fixed to constraints imposed by the Dunham model. The Dunham constants allow for the prediction of line positions with high J. In order to predict the line positions of GaH and GaD with high v an internuclear potential energy function was determined. This was achieved by a direct fit of the spectral data to the eigenvalues of an effective radial Schrödinger equation containing a parameterized internuclear potential energy function.

ACKNOWLEDGMENTS

This work was supported by the Phillips Laboratory/Propulsion Directorate, Edwards Air Force Base, California, and the Natural Science and Engineering Research Council of Canada (NSERC). Acknowledgement is made to the Petroleum Research Fund, administered by the American Chemical Society, for partial support of this work. We thank J. Ogilvie for providing us with his list of constrained U_{ij} relations.

[1] J. B. White, M. Dulick, and P. F. Bernath, J. Chem. Phys. **99**, 8371 (1993).
[2] W. R. Garton, Proc. Phys. Soc. A **64**, 507 (1951).
[3] H. Neuhaus, Ark. Fys. **14**, 551 (1958).
[4] H. Neuhaus, Nature **180**, 434 (1957).
[5] M. Kronekvist, A. Lagerqvist, and H. Neuhaus, J. Mol. Spectrosc. **39**, 516 (1971).
[6] M. L. Ginter and K. K. Innes, J. Mol. Spectrosc. **7**, 64 (1961).
[7] P. C. Poyner, K. K. Innes, and M. L. Ginter, J. Mol. Spectrosc. **23**, 237 (1967).
[8] G. Lakshminarayana and B. J. Shetty, J. Mol. Spectrosc. **122**, 417 (1987).
[9] M. L. Ginter and R. Battino, J. Chem. Phys. **42**, 3222 (1965).
[10] L. G. M. Pettersson and S. R. Langhoff, J. Chem. Phys. **85**, 3130 (1986).
[11] G.-B. Kim and K. Balasubramanian, J. Mol. Spectrosc. **134**, 412 (1989).
[12] R.-D. Urban, U. Magg, and H. Jones, Chem. Phys. Lett. **154**, 135 (1989).
[13] R.-D. Urban, H. Birk, P. Polomsky, and H. Jones, J. Chem. Phys. **94**, 2523 (1991).
[14] C. I. Frum, R. Engleman, and P. F. Bernath, J. Chem. Phys. **93**, 5457 (1990).
[15] K. A. Walker, H. G. Hedderich, and P. F. Bernath, Mol. Phys. **78**, 577 (1993).
[16] H. G. Hedderich, M. Dulick, and P. F. Bernath, J. Chem. Phys. **99**, 8363 (1993).
[17] R. A. Toth, J. Opt. Soc. Am. B **8**, 2236 (1991).
[18] See AIP document no. PAPS JCPSA-99-8379-12 for the 12 pages of tables. Order by PAPS number and journal reference from American Institute of Physics, Physics Auxiliary Publication Service, 500 Sunnyside Boulevard, Woodbury, New York 11797-2999. The price is $1.50 for each microfiche (60 pages) or $5.00 for photocopies of up to 30 pages, and $0.15 for each additional page over 30 pages. Airmail additional. Make checks payable to the American Institute of Physics.
[19] J. L. Dunham, Phys. Rev. **41**, 721 (1932).
[20] J. K. G. Watson, J. Mol. Spectrosc. **80**, 411 (1980).
[21] J. K. G. Watson, J. Mol. Spectrosc. **45**, 99 (1973).
[22] J. Ogilvie (private communication); Comput. Phys. Commun. **30**, 101 (1983).
[23] M. Dulick and P. F. Bernath (in preparation).
[24] J. A. Coxon and P. G. Hajigeorgiou, Can. J. Phys. **70**, 40 (1992).
[25] J. A. Coxon and P. G. Hajigeorgiou, Chem. Phys. **167**, 327 (1992).
[26] K. P. Huber and G. Herzberg, *Constants of Diatomic Molecules* (Van Nostrand–Reinhold, New York, 1979).
[27] I. Mills, *Quantities, Units, and Symbols in Physical Chemistry* (Blackwell, Oxford, 1989).